

# Light Scattering from Poly(L-glutamic acid) in Aqueous Solution in the Helix-Coil Transition Region

Akinori Kidera and Akio Nakajima\*

Department of Polymer Chemistry, Kyoto University, Kyoto 606, Japan.

Received June 18, 1983

**ABSTRACT:** The helix-coil transition of poly(L-glutamic acid) (PGA) in aqueous solution was investigated by light scattering measurement. In the coil state at neutral pH,  $z$ -average mean square radii of gyration  $\langle S^2 \rangle_z$  and second virial coefficients  $A_2$  were obtained at several added salt concentrations. Their dependences on added salt concentration show that PGA in the coil state behaves as a typical polyelectrolyte, and their numerical values, which are larger than those of vinyl polyelectrolytes, indicate that the coil conformation of PGA is a fairly extended structure. In the helix-coil transition region at acidic pH,  $\langle S^2 \rangle_z$  was obtained by using isoionic buffer solutions of various pH values and two added salt concentrations. The experimental results show a decrease in  $\langle S^2 \rangle_z$  with increasing helical fraction  $\theta_h$  up to  $\theta_h \approx 0.5$ , which is contrary to the case of neutral poly(amino acids). Such a feature can also be attributed to the extended coil structure. Thus, the effect of electrostatic interaction on the conformation of a poly(amino acid) mainly leads to the extended coil structure both in the coil state and in the transition region.

The molecular dimensions of neutral poly(amino acids) in the helix-coil transition region can be described by the Miller-Flory model,<sup>1</sup> in which the rotational isomeric state approximation<sup>2</sup> is extended to poly(amino acids) in the transition region. In many cases, even a simplified Nagai model,<sup>3</sup> in which rigid rods and random flight chains are connected alternately, is sufficient to analyze the experimental results.<sup>4</sup> These facts imply that the unperturbed chain model suffices to describe the dimensional change of neutral poly(amino acids) in the transition region.

On the other hand, for ionizable poly(amino acids), it becomes much more difficult to interpret the dimensional change in the transition region because of electrostatic interaction due to charges on the side chains. Ptitsyn et al.<sup>5</sup> studied the molecular dimensions of poly(L-glutamic acid) and poly(L-lysine) in the transition region through the intrinsic viscosity  $[\eta]$ . In the viscometric measurements of polyelectrolytes, however, there remains a problem that  $[\eta]$  does not directly reflect the molecular dimensions.<sup>6</sup>

In the present study, the molecular dimensions of poly(L-glutamic acid) (PGA) in aqueous solution are measured by light scattering to avoid the problem in  $[\eta]$ . It is discussed how electrostatic interaction due to charges on the side chains influences the molecular dimensions of a poly(amino acid) in the helix-coil transition region. First, the experimental results on the coil conformation in the fully ionized state are reported in terms of the ionic strength dependence. Second, the dimensional change in the transition region is discussed in terms of the degree of ionization.

## Experimental Section

**Materials.** Two samples of poly(L-glutamic acid) (PGA) were obtained by debenzoylation of poly( $\gamma$ -benzyl L-glutamate), which was synthesized by the method described previously.<sup>7</sup> Each sample of PGA was purified in a Na salt form by precipitating twice by using 1 N NaCl aqueous solution as the solvent and a 2:1 acetone-methanol mixture as the precipitant and was further fractionated in an acidic form into three fractions with dimethyl sulfoxide as the solvent and 2-propanol as the precipitant. Finally, these fractions were dialyzed against pure water and freeze-dried.

All the measurements were carried out with the middle fraction of the two samples designated as PGA I and PGA II, of which weight-average molecular weights  $M_w$  measured by light scattering were  $(1.12 \pm 0.06) \times 10^5$  and  $(1.04 \pm 0.05) \times 10^5$ , respectively. PGA I and PGA II were used for the measurements in the coil state and in the transition region, respectively. The complete absence of the  $\gamma$ -benzyl group in PGA was confirmed by lack of absorption near 260 nm, where the benzyl ester chromophore absorbs, using a Hitachi EPS-3T recording spectrophotometer. It should be

noted that even a small amount of residual benzyl group changes the conformational properties of PGA.<sup>8,9</sup>

**Potentiometric Titration.** Potentiometric titrations were carried out by the method described previously.<sup>7</sup>

**Light Scattering Measurement.** Scattering intensity was measured by a Sofica Fica 50 automatic light scattering photometer at angles from 45° to 150° with polarized light of 546 nm. The Rayleigh ratio for benzene at 25 °C,  $16.0 \times 10^{-6}$  at 546 nm,<sup>10,11</sup> was used for the calibration constant of the photometer. As the added salt for the solution, NaCl was used at neutral pH, and an isoionic buffer solution composed of sodium acetate-acetic acid-KCl was used at acidic pH. The latter was chosen because PGA at acidic pH changes its conformation sensitively with small changes in pH. Changes in pH during the measurements at neutral and acidic pH were less than  $\pm 0.1$  and  $\pm 0.01$  pH unit, respectively. Concentrations were determined by conductometric titration using a Yanagimoto MY-8 conductivity outfit. For the range of polymer concentration in light scattering measurements,  $2 \times 10^{-4}$ – $7 \times 10^{-4}$  g/mL was chosen to avoid anomalous scattering in a solution of high polyion concentration and low salt concentration.<sup>12</sup> Solutions were clarified by filtration through a Millipore filter HA (0.45- $\mu$ m pore size) followed by centrifugation at  $6 \times 10^4g$  for 2 h using a Marusan centrifuge 50S. The refractive index increments for the solution dialyzed against the solvent  $(d\tilde{n}/dc)_u$ , were measured by a Union Giken RM-101 differential refractometer. The values of  $(d\tilde{n}/dc)_u$  at neutral pH were found to be 0.170, 0.183, 0.190, 0.194, and 0.195 for added salt concentrations  $c_s$  of 0.5, 0.2, 0.1, 0.05, and 0.02, respectively. Data analyses were done by the method reported by Hara and Nakajima.<sup>12</sup>

## Results and Discussion

**Coil State.** A typical example of a Zimm plot for PGA in aqueous solution is shown in Figure 1, which includes data from quadruplicate experiments on the PGA I-0.1 N NaCl system at 25.0 °C. The values at zero polymer concentration were obtained from the square root plots. Optical anisotropy of all the solutions was found to be negligibly small. Zimm plots for various added salt concentrations  $c_s$  did not show any anomalous inflection in the  $Kc/R_\theta(\theta = 0)$  vs.  $c$  curve which is seen in a solution of high polyion concentration and low added salt concentration.<sup>12</sup>  $z$ -average mean square radii of gyration  $\langle S^2 \rangle_z$  and second virial coefficients  $A_2$  at various added salt concentrations were obtained from the initial slopes of the  $Kc/R_\theta(c = 0)$  vs.  $\sin^2(\theta/2)$  curves and the  $Kc/R_\theta(\theta = 0)$  vs.  $c$  curves, respectively. The results are summarized in Table I together with the values of  $A_2$  obtained from experiments on PGA II.

$c_s$  dependences on the dimensions and  $A_2$  are shown in Figure 2, in which a linear relationship between  $\langle S^2 \rangle_z^{3/2}$  and  $c_s^{-1/2}$  is found and in which  $A_2$  is shown to be pro-

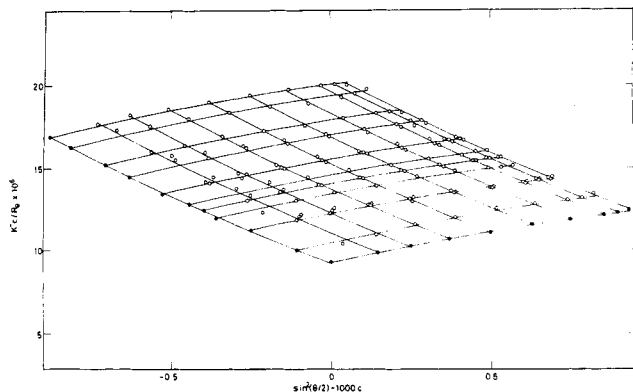


Figure 1. Zimm plot for the PGA I ( $M_w = 1.12 \times 10^6$ )-0.1 N NaCl system at pH 7.0.

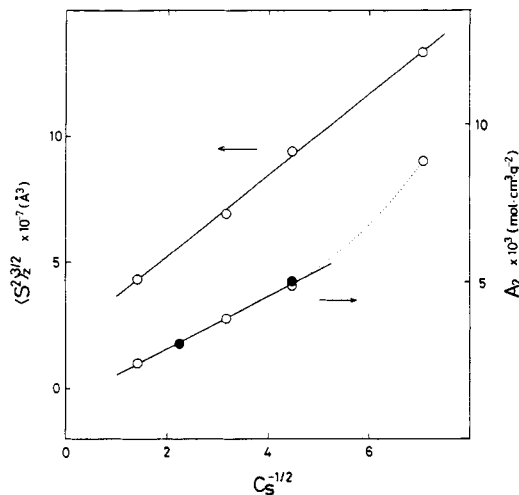


Figure 2. Plots of  $\langle S^2 \rangle_z^{3/2}$  and  $A_2$  against  $c_s^{-1/2}$ . The unfilled circles are data for PGA I and the filled circles are those for PGA II.

Table I  
Light Scattering Data for PGA I-NaCl Aqueous Solutions ( $M_w = 1.12 \times 10^5$ )

$c_s$ , N	$\langle S^2 \rangle_z^{1/2}$ , Å	$A_2 \times 10^3$ , (mol·cm <sup>3</sup> )/g <sup>2</sup>
0.5	350 ± 30	2.4 ± 0.1
0.2		3.0 ± 0.2 <sup>a</sup>
0.1	410 ± 30	3.8 ± 0.2
0.05	455 ± 40	4.8 ± 0.3, 5.0 ± 0.3 <sup>a</sup>
0.02	510 ± 40	8.8 ± 0.5

<sup>a</sup> Data of PGA II ( $M_w = 1.04 \times 10^5$ ).

portional to  $c_s^{-1/2}$  at high  $c_s$  and to be proportional to  $c_s^{-1}$  at low  $c_s$ . The fact that these linear relationships on  $c_s$  are those of typical polyelectrolytes<sup>13,14</sup> indicates that the PGA coil in aqueous solution behaves as a typical polyelectrolyte. Hawkins and Holtzer<sup>15</sup> obtained the same  $c_s$  dependence of  $A_2$  in PGA aqueous solutions, i.e., a linear relationship between  $A_2$  and  $c_s^{-1/2}$  at  $c_s = 0.1$ -1.0. Further,  $[\eta]$  of PGA have given the  $c_s$  dependence of typical polyelectrolytes, a linear relationship between  $[\eta]$  and  $c_s^{-1/2}$ .<sup>15,16</sup>

However, the numerical values shown in Table I are larger than those for vinyl polyelectrolytes.<sup>6,12,17-22</sup> According to Brant and Flory,<sup>23</sup> the radius of gyration of PGA I in the unperturbed state  $\langle S_0^2 \rangle_z$  is estimated at 150 Å,<sup>24</sup> and expansion factors  $\alpha_s$  for the data in Table I become 2.3, 2.7, 3.0, and 3.4 at  $c_s = 0.5, 0.1, 0.05$ , and 0.02, respectively. The values of  $A_2$  are much larger than those of poly(acrylic acid)<sup>12</sup> and almost comparable to those of (carboxymethyl)cellulose<sup>25</sup> and hyaluronic acid,<sup>26</sup> which have stiff backbones.<sup>27</sup> These results agree qualitatively

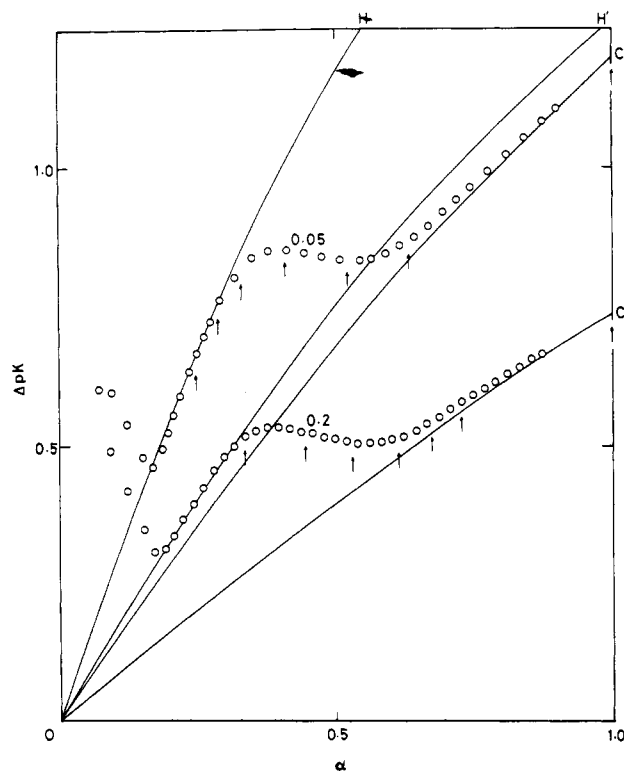


Figure 3. Potentiometric titration curves of PGA II.  $\Delta pK = pK - pK_0$ , where  $pK_0$ , the intrinsic ionization constant, is 4.525 and 4.495 for  $c_s = 0.05$  and 0.2, respectively. Solid curves were calculated by assuming a rod model (radius  $r_s$  (Å)) and uniform smeared charge density (number of charges per unit length  $\nu$  (Å<sup>-1</sup>)).<sup>7</sup>  $r_s = 14.0$  and  $1/\nu = 1.5$  for curves OH and OH';  $r_s = 10.7$  and  $1/\nu = 3.6$  for curve OC';  $r_s = 11.5$  and  $1/\nu = 3.6$  for curve OC'. Arrows indicate the points at which the light scattering measurements were carried out.

with the results of viscometric studies, in which fairly large  $a$  values of the Mark-Houwink-Sakurada equation  $[\eta] = KM^a$  were reported.<sup>15,16,28</sup> Therefore, it is concluded that the electrostatic interaction extends a PGA chain much more than expected in vinyl polymers.

**Helix-Coil Transition Region.** Light scattering from a poly(amino acid) in the helix-coil transition region gives an apparent value of the mean square radius of gyration  $\langle S^2 \rangle_{app}$  because of the copolymer nature,<sup>29</sup> as being represented by the difference in refractive index increment between coil and helix residues. However, Teramoto et al.<sup>30</sup> concluded from their calculation using the Nagai model<sup>3</sup> that the copolymer nature of neutral poly(amino acids) in the transition region scarcely affects the light scattering measurements of molecular dimensions. Further, Miller and Flory's model<sup>1</sup> with an extended coil structure showed less than 3% difference between  $\langle S^2 \rangle_{app}$  and  $\langle S^2 \rangle$  at most (see Appendix). Although the above models do not include the electrostatic long-range interaction, the latter model may suffice for the purpose of checking the copolymer nature of PGA in the transition region because correlation in the sequence distribution of coil and helix states between distant segments may not be important in a system having a low cooperativity of the Zimm-Bragg parameter  $\sigma = 1 \times 10^{-3}$ .<sup>31</sup> Thus,  $\langle S^2 \rangle_{app}$  is equated to  $\langle S^2 \rangle$  in the following discussion.

Light scattering measurements on PGA II at two added salt concentrations were carried out at various degrees of ionization  $\alpha$  indicated by arrows in Figure 3. The helical fraction  $\theta_h$  at each  $\alpha$  was obtained from potentiometric titration data by the method described previously.<sup>7</sup> It is noted that the value of  $\Delta pK$  in Figure 3, which is char-

Table II  
Light Scattering and Potentiometric Titration Data for  
PGA II ( $M_w = 104\,000$ ) in the Helix-Coil  
Transition Region

$I = 0.05$				$I = 0.2$			
pH	$\alpha$	$\theta_h$	$\langle S^2 \rangle_z^{1/2}, \text{\AA}$	pH	$\alpha$	$\theta_h$	$\langle S^2 \rangle_z^{1/2}, \text{\AA}$
7	1.0	0.0	460	7	1.0	0.0	360
5.62	0.63	0.06	420	5.50	0.73	0.02	330
5.40	0.52	0.22	390	5.35	0.68	0.04	310
5.22	0.41	0.65	360	5.21	0.61	0.09	290
5.03	0.33	0.88	320	5.05	0.53	0.24	270
4.86	0.29	0.95	290	4.92	0.45	0.53	260
4.68	0.25	0.98		4.72	0.34	0.84	

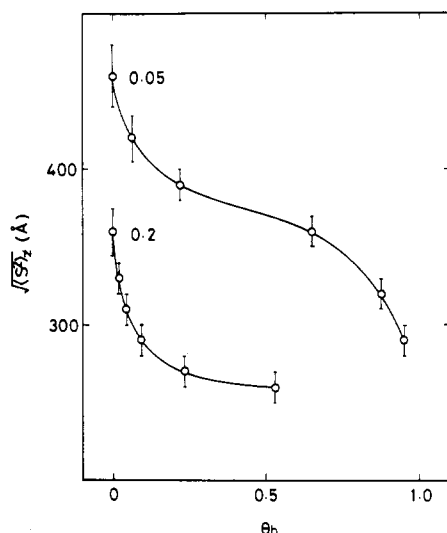


Figure 4. Dependence of  $\langle S^2 \rangle_z^{1/2}$  on the helical fraction  $\theta_h$ . The error symbols reflect errors in determining  $\langle S^2 \rangle_z$  from the initial slope of the  $Kc/R_\theta(c=0)$  vs.  $\sin^2(\theta/2)$  curve.  $\langle S^2 \rangle_z$  at  $\theta_h = 1$  was estimated at 450 Å.<sup>24</sup>

acteristic of the electrostatic potential near a polyion surface, is almost constant in the transition region. Hence, it is found that the electrostatic interaction is almost constant through the transition region and that dimensional change may be attributed only to changes in helical fraction  $\theta_h$ . In Table II, the results of  $\langle S^2 \rangle_z$  in the transition region are summarized together with those of  $\alpha$  and  $\theta_h$ . At the lowest pH in Table II,  $\langle S^2 \rangle_z$  was not able to be obtained because of intermolecular aggregation.<sup>32</sup>

$\langle S^2 \rangle_z^{1/2}$  is plotted against  $\theta_h$  in Figure 4, in which the molecular dimensions show a contraction in the course of the coil-to-helix transition. However, it is expected that  $\langle S^2 \rangle_z$  passes through a minimum as  $\theta_h$  goes to 1 since  $\langle S^2 \rangle_z$  at  $\theta_h = 1$  is estimated at 450 Å.<sup>24</sup> This feature clearly shows a difference from the results for neutral poly(amino acids), poly( $\gamma$ -benzyl L-glutamate) (PBLG),<sup>33</sup> and poly( $N^5$ -(hydroxypropyl)-L-glutamine) (PHPG),<sup>34</sup> for which  $\langle S^2 \rangle_z$  increase monotonously as  $\theta_h$  increases.

There are two important factors which determine the  $\theta_h$  dependence of the dimensions in the transition region, that is, the difference in the contour length of a chain from the coil ( $=3.8$  Å/residue) to  $\alpha$ -helix ( $=1.5$  Å/residue) and the difference in the flexibility of a chain from the flexible coil to rigid  $\alpha$ -helix. In the course of the coil-to-helix transition, the former makes the dimensions smaller and the latter works oppositely. Low cooperativity or extended (or less flexible) coil structure reduces the latter effect. Actually, a neutral poly(amino acid), poly( $N^5$ -(hydroxyethyl)-L-glutamine) (PHEG),<sup>35</sup> having 10 times lower cooperativity than PBLG and PHPG,<sup>36</sup> which is the same order as that of PGA, shows a minimum in the  $\langle S^2 \rangle_z$  vs.

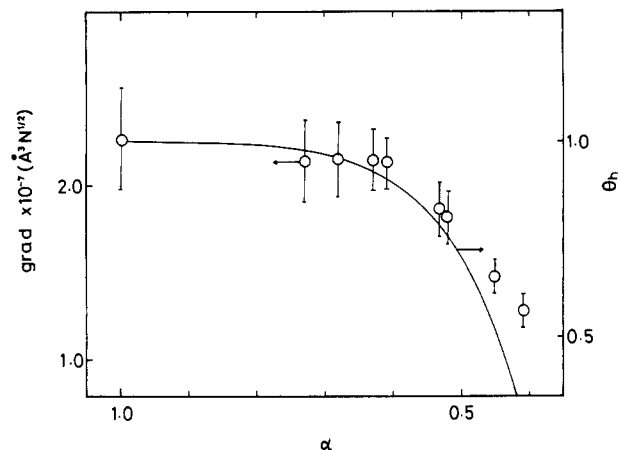


Figure 5. Gradient of the plot of  $\langle S^2 \rangle_z^{3/2}$  vs.  $c_s^{-1/2}$  plotted against  $\alpha$ . The error symbols are the same as those in Figure 4. The solid curve is the plot of  $\theta_h$  against  $\alpha$ .

$\theta_h$  curve. However, since the minimum of PHEG is very shallow and the dimensions increase when  $\theta_h \geq 0.5$ , the contraction of PGA up to  $\theta_h \geq 0.5$  should be attributed not only to its low cooperativity but also to the extended coil structure shown in the preceding section.

Hence, it is concluded that the electrostatic interaction, which makes the  $\theta_h$  dependence of the dimensions shown in Figure 4, mainly leads to the extended coil structure as similarly shown in the data on the coil state. This conclusion is supported by the  $c_s$  dependence of the dimensions. By assuming that the  $c_s$  dependence of the dimensions in Figure 2 holds also in the transition region, the effects of electrostatic interaction on the dimensions can be examined from the gradient of the plot of  $\langle S^2 \rangle_z^{3/2}$  vs.  $c_s^{-1/2}$ . In Figure 5, the gradient,  $[\langle S^2 \rangle_z^{3/2}(c_s = 0.05) - \langle S^2 \rangle_z^{3/2}(c_s = 0.2)] / [(0.05)^{-1/2} - (0.2)^{-1/2}]$ , is plotted against  $\alpha$ . The decrease in the gradient accompanied with the decrease in the coil fraction indicates that the effect of electrostatic interaction on the dimensions appears mainly in the coil dimensions.

However, further contraction in  $c_s = 0.05$  at  $\theta_h$  close to 1 suggests that there may be an attractive interaction between two helix sequences in a chain, which was mentioned above as the cause of the intermolecular aggregation even at high charge density.

**Acknowledgment.** We are indebted to Dr. M. Hara for advice on light scattering measurements and helpful discussion.

#### Appendix. Apparent Radius of Gyration of a Poly(amino acid) in the Helix-Coil Transition Region

The apparent radius of gyration is given in a generator matrix formulation<sup>37</sup> using the Miller-Flory model<sup>1</sup> by

$$\langle S^2 \rangle_{\text{app}} = (N+1)^{-2} \psi^{-2} \sum_{0 \leq i < j \leq n} \psi_i \psi_j \langle r_{ij}^2 \rangle = \frac{(N+1)^{-2} \psi^{-2} Z^{-1} \mathbf{F}_1 \mathbf{F}^{N-2} \mathbf{F}_1}{(N+1)^{-2} \psi^{-2} Z^{-1} \mathbf{F}_1 \mathbf{F}^{N-2} \mathbf{F}_1} \quad (1)$$

with

$$\mathbf{F} = (\mathbf{U} \otimes \mathbf{E}_2) \|\mathbf{S}\|$$

$$\mathbf{F}_1 = (\mathbf{S}_1 \quad \mathbf{O})$$

and

$$\mathbf{F}_1 = \begin{pmatrix} \mathbf{S}_1 \\ \mathbf{S}_1 \end{pmatrix}$$

where  $N$  is the degree of polymerization, the partition function  $Z$  is given by

$$Z = (1 \quad 0)U^N \begin{pmatrix} 1 \\ 1 \end{pmatrix}$$

with

$$U = \begin{pmatrix} 1 & \sigma s \\ 1 & s \end{pmatrix} \quad (2)$$

$s$  and  $\sigma$  are the Zimm-Bragg parameters, the generator matrix of the  $i$ th residue  $S_i$  is written in the form

$$S_i = \begin{bmatrix} 1 & \psi_{i-1} G_{[i} & \psi_{i-1} \psi_i d^z \\ 0 & G_i & \psi_i G_i] \\ 0 & 0 & 1 \end{bmatrix} \quad (3)$$

with

$$G_i = \begin{bmatrix} 1 & 2d^T T_i & d^z \\ 0 & T_i & d \\ 0 & 0 & 1 \end{bmatrix}$$

and

$$\|S\| = \begin{bmatrix} S_c & 0 \\ 0 & S_h \end{bmatrix}$$

subscripts  $c$  and  $h$  mean coil and helix states, respectively,  $E_2$  is a  $2 \times 2$  identity matrix,  $S_i$  and  $S_j$  are the first row and the last column vector of  $S$ , respectively, and  $G_{[i}$  and  $G_i]$  are defined in the same way from  $G_i$ .  $\psi$  is the mean value of refractive index increment defined as

$$\psi = (1 - \theta_h)\psi_c + \theta_h\psi_h \quad (4)$$

where  $\psi_c$  and  $\psi_h$  depend on the degree of ionization  $\alpha$  and are written as

$$\psi_c = (1 - \alpha)m^0\psi_c^0 + \alpha m^-\psi_c^-$$

$$\psi_h = (1 - \alpha)m^0\psi_h^0 + \alpha m^-\psi_h^-$$

$m^0$  and  $m^-$  are the molecular weights of uncharged and charged residues, respectively, and  $\psi_c^0$ ,  $\psi_c^-$ ,  $\psi_h^0$ , and  $\psi_h^-$  are the refractive index increments of uncharged and charged residues in the coil and helix states, respectively.  $d$  is the virtual bond vector between adjacent  $\alpha$ -carbons, and the transformation matrix  $T_i$  and refractive index increment  $\psi_i$  for the  $i$ th residue are given by

$$T_i = \langle T_c \rangle; \quad \psi_i = \psi_c$$

for the  $i$ th residue in a coil state and

$$T_i = T_h; \quad \psi_i = \psi_h$$

for the  $i$ th residue in a helix state, where  $\langle T_c \rangle$  is the average transformation matrix for the coil state and  $T_h$  is the transformation matrix for the right-handed  $\alpha$ -helix. The real value  $\langle S^2 \rangle$  is given by setting  $\psi_c = \psi_h$ . The parameters used in the calculation were  $N = 514$ ,  $\sigma = 1 \times 10^{-3}$ , and  $\psi_h/\psi_c = 2$ , and the average transformation matrices of L-alanine<sup>38</sup> and L-proline<sup>39</sup> were used for  $\langle T_c \rangle$ . The latter was adopted as a model for the extended coil structure.

The maximum difference between  $\langle S^2 \rangle_{app}$  and  $\langle S^2 \rangle$  was estimated at 1.4% at  $\theta_h = 0.85$  and 2.6% at  $\theta_h = 0.50$  for the case of using  $\langle T_c \rangle$  of L-alanine and that of L-proline, respectively.

**Registry No.** Poly(L-glutamic acid) (homopolymer), 25513-46-6; poly(L-glutamic acid) (SRU), 24991-23-9.

## References and Notes

- (1) Miller, W. G.; Flory, P. J. *J. Mol. Biol.* **1966**, *15*, 298.
- (2) Flory, P. J. "Statistical Mechanics of Chain Molecules"; Wiley-Interscience: New York, 1969.
- (3) Nagai, K. *J. Chem. Phys.* **1961**, *34*, 887.
- (4) Teramoto, A.; Fujita, H. *Adv. Polym. Sci.* **1975**, *18*, 65.
- (5) Bychkova, V. E.; Ptitsyn, O. B.; Barskaya, T. V. *Biopolymers* **1971**, *10*, 2161. Barskaya, T. V.; Ptitsyn, O. B. *Ibid.* **1971**, *10*, 2181.
- (6) Takahashi, A.; Kato, T.; Nagasawa, M. *J. Phys. Chem.* **1967**, *71*, 2001.
- (7) Kidera, A.; Nakajima, A. *Macromolecules* **1981**, *14*, 640.
- (8) Rao, S. P.; Miller, W. G. *Biopolymers* **1973**, *12*, 835.
- (9) By light scattering measurements, second virial coefficients  $A_2$  of PGA having a few percent of residual benzyl groups at neutral pH were found to be much smaller than those of PGA I and PGA II shown in Table I;  $A_2 \times 10^3 = 1.0, 2.5, 4.0$ , and  $6.8$  at  $c_s = 0.5, 0.1, 0.05$ , and  $0.02$ , respectively.
- (10) Coumou, D. J. *J. Colloid Sci.* **1960**, *15*, 408.
- (11) Deželić, G. *J. Chem. Phys.* **1966**, *45*, 185.
- (12) Hara, M.; Nakajima, A. *Polym. J.* **1980**, *12*, 693, 703.
- (13) Noda, I.; Tsuge, T.; Nagasawa, M. *J. Phys. Chem.* **1970**, *74*, 710.
- (14) Nagasawa, M.; Takahashi, A. In "Light Scattering from Polymer Solutions"; Huglin, M. B., Ed.; Academic Press: New York, 1972; p 671.
- (15) Hawkins, R. B.; Holtzer, A. *Macromolecules* **1972**, *5*, 294.
- (16) Satoh, M.; Komiyama, J.; Iijima, T. *Colloid Polym. Sci.* **1980**, *258*, 136.
- (17) Orofino, T. A.; Flory, P. J. *J. Phys. Chem.* **1959**, *63*, 283.
- (18) Eisenberg, H.; Woodside, D. *J. Chem. Phys.* **1962**, *36*, 1844.
- (19) Raziel, A.; Eisenberg, H. *Isr. J. Chem.* **1973**, *11*, 183.
- (20) Tan, J. S.; Gasper, S. P. *J. Polym. Sci., Polym. Phys. Ed.* **1974**, *12*, 1785; **1975**, *13*, 1705.
- (21) Fisher, L. W.; Sochor, A. R.; Tan, J. S. *Macromolecules* **1977**, *10*, 949.
- (22) Kitano, T.; Taguchi, A.; Noda, I.; Nagasawa, M. *Macromolecules* **1980**, *13*, 57.
- (23) Brant, D. A.; Flory, P. J. *J. Am. Chem. Soc.* **1965**, *87*, 2788.
- (24) The characteristic ratio of PGA was reported as  $8.8^{23}$   $\langle S^2 \rangle^{1/2}$  of PGA I in the unperturbed state is given by  $\langle S_0^2 \rangle^{1/2} = [(8.8/6)(M_w/M_0)(h+2)/(h+1)d_c^2]^{1/2} \sim 150$  Å, where  $M_0$  is the molecular weight of a sodium glutamate residue ( $=151.1$ ),  $h = M_n/(M_w - M_n)$ ,  $M_n$  is the number-average molecular weight (here we put  $h = 1$ ), and  $d_c$  is the virtual bond length ( $=3.8$  Å). In the same way,  $\langle S^2 \rangle^{1/2}$  of PGA II in the complete helix state is given by  $\langle S^2 \rangle^{1/2} = (1/12)^{1/2}(M_w/M_0)(h+2)/(h+1)d_h \sim 450$  Å, where  $d_h$  is the pitch of the  $\alpha$ -helix ( $=1.5$  Å).
- (25) Schneider, N. S.; Doty, P. *J. Phys. Chem.* **1954**, *58*, 762.
- (26) Cleland, R. L. *Biopolymers* **1968**, *6*, 1519.
- (27) Second virial coefficients  $A_2$  of poly(acrylic acid) ( $M_w = 5.0 \times 10^5$ ) in NaCl aqueous solutions<sup>12</sup> are  $2.8 \times 10^{-4}$ ,  $1.3 \times 10^{-3}$ , and  $8.8 \times 10^{-3}$  (mol-cm<sup>3</sup>)/g<sup>2</sup> at  $c_s = 1.0, 0.1$ , and  $0.01$ , respectively.  $A_2$  of (carboxymethyl)cellulose ( $M_w = 4.4 \times 10^5$ ) in NaCl aqueous solutions<sup>26</sup> were reported as  $1.51 \times 10^{-3}$ ,  $5.70 \times 10^{-3}$ ,  $15.7 \times 10^{-3}$ , and  $26.0 \times 10^{-3}$  at  $c_s = 0.5, 0.05, 0.01$ , and  $0.005$ , respectively.  $A_2$  of hyaluronic acid ( $M_w = 3.1 \times 10^5$ ) in NaCl aqueous solutions<sup>26</sup> were  $1.3 \times 10^{-3}$ ,  $1.4 \times 10^{-3}$ ,  $3.3 \times 10^{-3}$ , and  $7.7 \times 10^{-3}$  at  $c_s = 2.0, 0.5, 0.1$ , and  $0.01$ , respectively.
- (28) Morcellet, M.; Loucheux, C. *Biopolymers* **1976**, *15*, 1857.
- (29) Benoit, H.; Froelich, D. In ref 14, p 467.
- (30) Teramoto, A.; Norisuye, T.; Fujita, H. *Polym. J.* **1970**, *1*, 55.
- (31) It was found that the value of  $\sigma$  is almost independent of both  $c_s$  and  $\alpha$ ;  $\sigma = 1.1 \times 10^{-3}$ ,  $1.5 \times 10^{-3}$ , and  $1.0 \times 10^{-3}$  at  $c_s = 0.05, 0.1$ , and  $0.2$ , respectively. The data of  $c_s = 0.1$  is from ref 7. Independency on  $\alpha$  was confirmed by the same method as described previously.<sup>7</sup>
- (32) Light scattering measurements showed that  $M_w$  of aggregated systems for both  $c_s = 0.05$  and  $0.2$  were almost twice as large as  $M_w$  of PGA II. It is also noted that the average contour distance between the adjacent charges at the lowest pH values in Table II is only 5–6 Å. This intermolecular aggregation at such a high charge density suggests that there is a strong affinity between the helix sequences of PGA.
- (33) Norisuye, T.; Teramoto, A.; Fujita, H. *Polym. J.* **1973**, *4*, 323.
- (34) Okita, K.; Teramoto, A.; Fujita, H. *Polym. J.* **1970**, *1*, 582.

- (35) Ohta, T.; Teramoto, A.; Fujita, H. *Polym. J.* 1976, 8, 281.  
 (36)  $\sigma$  values of PBLG, PHPG, and PHEG are  $9.0 \times 10^{-5}$ ,  $3.2 \times 10^{-4}$ , and  $(1.5-4.4) \times 10^{-3}$ .<sup>33-35</sup>  
 (37) Flory, P. J. *Macromolecules* 1974, 7, 381.  
 (38) Conrad, J. C.; Flory, P. J. *Macromolecules* 1976, 9, 41.  
 (39) Schimmel, P. R.; Flory, P. J. *Proc. Natl. Acad. Sci. U.S.A.* 1967, 58, 52.  $\langle T_c \rangle$  of L-proline in this reference suffices for the model of the extended coil structure, but cannot give a correct unperturbed dimension of poly(L-proline); see: Tanaka, S.; Scheraga, H. A. *Macromolecules* 1975, 8, 623.

## Investigation of the Chain Conformation in Uniaxially Stretched Poly(dimethylsiloxane) Networks by Small-Angle Neutron Scattering

Michel Beltzung, Claude Picot, and Jean Herz\*

Centre de Recherches sur les Macromolécules (CNRS), 67083 Strasbourg, France.  
 Received May 19, 1983

**ABSTRACT:** The behavior of network chains in dry poly(dimethylsiloxane) networks submitted to uniaxial extension was investigated by small-angle neutron scattering. The measurements were carried out on "end-linked" networks. The experimental results were compared with those expected on the basis of the models proposed by the classical theories of rubber elasticity, but the observed behavior at the level of the elastic chain cannot be interpreted within the framework of a unique model. An interpretation of the chain behavior, taking into account a rearrangement of cross-link positions upon deformation, is proposed.

### I. Introduction

In spite of very intensive theoretical and experimental investigations, many questions concerning the behavior of elastic chains in rubber networks remain open or are still subject to controversy. Therefore the study of the network behavior at a molecular level in relation to the structural characteristics of the system is of major interest.

A previous article was devoted to an investigation by small-angle neutron scattering (SANS) of poly(dimethylsiloxane) (PDMS) networks in the dry undeformed state;<sup>1</sup> it was shown that upon cross-linking in the bulk by an end-linking process involving a polymer precursor, the chain dimensions remain unchanged. On the other hand, no memory effect or supercoiling of the elastic chains could be observed.

A macroscopic deformation of the network, either by swelling in a solvent or by mechanical constraint, induces a displacement of the cross-links and thus gives rise to a deformation of the elastic chains attached to the latter. An investigation by SANS of the behavior of the elastic chains in PDMS networks upon swelling in a thermodynamically good solvent has been published recently.<sup>2</sup>

The present article is focused on a study of dry PDMS networks submitted to uniaxial extension. Again, SANS is a powerful technique to characterize the deformation of the elastic chains that results from a macroscopic deformation of the system. The scattering experiments were carried out on samples on which the stress-strain behavior was determined simultaneously.

### II. Theory

The deformation ratio of a network submitted to a uniaxial extension parallel to the Oz axis is defined by  $\lambda_z = \lambda = L/L_i$ , where  $L$  and  $L_i$  are the lengths of the deformed and undeformed sample. Generally, one assumes that deformation occurs at constant volume:  $\lambda_x = \lambda_y = \lambda_z^{-1/2}$ . The corresponding elastic force is given by

$$F = \left( \frac{\delta A_{el}}{\delta L} \right)_{T, \nu} = \left( \frac{\delta A_{el}}{\delta \lambda} \right)_{T, \nu} \frac{1}{L_i} \quad (1)$$

$A_{el}$  is the elastic free energy of the system.

In the earliest theories of rubber elasticity<sup>3-7</sup> the cross-links were considered to be firmly embedded in the

elastomeric polymer matrix. This implies that in the deformed sample the displacement of these cross-links is affine in the macroscopic deformation.

The elastic energy was calculated in the case of Gaussian chains.<sup>8</sup> To define the elastic free energy, a reference state was considered, in which the mean square end-to-end distance of the elastic chains is the same as that of the unperturbed free chains. According to experiments reported earlier,<sup>1</sup> this can be considered to be true for undeformed dry networks. Under these hypotheses the stress  $\sigma$  and the shear modulus  $G$  are given by

$$\sigma = \frac{F}{S_i} = \nu RT(\lambda - \lambda^{-2}) \quad (2)$$

$$G = \lim_{\lambda \rightarrow 1} \left( \frac{\sigma}{\lambda - \lambda^{-2}} \right) = \nu RT \quad (3)$$

where  $S_i$  is the cross section of the undeformed sample,  $\nu$  the number of network chains per unit volume,  $R$  the gas constant, and  $T$  the absolute temperature.

Another approach is based on the "phantom network" model of James and Guth.<sup>9,10</sup> These authors supposed that the network chains can move freely without any restriction due to neighboring chains. The elastic chains merely transmit the forces exerted upon the junctions. The chains are assumed to follow Gaussian statistics. Such a phantom network can be characterized as follows:<sup>9-11</sup> (i) the mean positions of the cross-links are defined by the macroscopic dimensions of the sample, (ii) the displacements of these mean positions are affine in the macroscopic deformation, and (iii) the fluctuations of the cross-links from their mean positions are Gaussian and their amplitude is independent of the deformation applied. Graessley<sup>12</sup> has calculated the elastic free energy and the strain corresponding to a deformation ratio  $\lambda$ :

$$\sigma = (\nu - \mu)RT(\lambda - \lambda^{-2}) \quad (4)$$

where  $\mu$  represents the number of cross-links per unit volume. The shear modulus of a phantom network is thus

$$G = (\nu - \mu)RT \quad (5)$$

This means that for a tetrafunctional network (where  $\nu/\mu = 2$ )  $G = 1/2\nu RT$ , half the shear modulus calculated in the